PUBLICATIONS OF THE
ASTRONOMICAL SOCIETY OF THE PACIFIC

Vol. 85 August 1973 No. 506

THE ROLE OF ROTATION IN CLOSE BINARY SYSTEMS OF HIGH MASS

RICHARD STOTHERS
Institute for Space Studies, Goddard Space Flight Center, NASA

Received 16 April 1973

A quantitative confrontation of theory and observation of massive close binary systems is presented in order to evaluate the role of axial rotation in the evolution of the individual stellar components as well as of the system as a whole. The detached systems are essentially unevolved, and possess components in approximately uniform rotation. The semidetached systems are definitely evolved, having suffered a heavy mass exchange before the stage of hydrogen exhaustion at the center of the original primary, and often possess mass-gaining components in fast nonuniform rotation. Except in the case of wide systems ($P > 2$ days), tidal friction eventually reinduces synchronism of rotation in both components and both components evolve inhomogeneously. Spin-down times of the envelope and core, total rotational angular momenta, and effects of spin-orbit interaction are calculated. A number of unexplained phenomena remain.

Key words: close binary systems — massive stars — stellar rotation — stellar evolution

I. Introduction

No systematic and detailed confrontation of theoretical predictions with observational data related to the axial rotation of stars in close binary systems has yet been made. Numerous specialized studies, particularly concerned with synchronization of the surface layers, are available but the interaction of rotation and evolution in these systems is largely unexplored (cf. Plavec 1970; van den Heuvel 1970). The question of uniform versus nonuniform rotation has been investigated recently, but only in a qualitative way (Stothers and Lucy 1972; Stothers 1972). In the present paper an attempt will be made to derive, from the available observational data for massive binary systems, a quantitative picture of the role of rotation in the evolution of these systems.

II. The Observational Data

Observational data are given in Table I for the members of 18 eclipsing binary systems in which at least one member has a spectral type in the range O–B4. Ziolkowski (1969) and van den Heuvel (1970) have found a natural division of all semidetached systems at a total system mass of $\sim 5\mathfrak{M}_\odot$, but another division of the individual components of detached and semidetached systems appears at a component mass of $\sim 3.5\mathfrak{M}_\odot$ (Devinney 1972). These two divisions correspond, respectively, to spectral types of B4–A0 and B7 for stars on the main sequence, and therefore all the systems of Table I lie in the massive group of systems. The format of Table I is as follows.

Columns (1) and (2): name and type of the system, where "d" and "s" refer to "detached" and "semidetached", respectively. Our assignment of type depends on whether or not one of the components, A or B, fills its Roche lobe, whose radius (in units of the orbital separation) is given approximately by

$$(R_A/a)_{crit} = 0.38 + 0.2 \log (\mathfrak{M}_A/\mathfrak{M}_B) \qquad (1)$$

for component A, and analogously for component B (Plavec 1968). Two assumptions necessary to compute the Roche lobe are (a) a circular orbit and (b) synchronous rotation of the components. These assumptions seem to be adequately satisfied for our present purposes.

TABLE I

OBSERVATIONAL DATA FOR EARLY TYPE ECLIPSING BINARY SYSTEMS

Binary (1)	Type (2)	P (days) (3)	Sp (4)	$\mathfrak{M}/\mathfrak{M}_\odot$ (5)	$R/R_\odot$ (cluster) (6)	$R/R_\odot$ (orbit) (7)	$R/R_\odot$ (gravity) (8)	$R/R_\odot$ (statistical) (9)	v (km sec^{-1}) (10)	v/v_{syn} (11)	R/a (12)	$(R/a)_{crit}$ (13)	M_{bol} (14)
AO Cas	sd	3.52	O9 III	19		13:	8.1:	16.3	160	0.86	0.38	0.35	−8.3
			O9 III	26		8.5:	8.1:	16.3	124	1.01	0.25	0.41	−7.3
λ Tau	sd	3.95	B3 V	6.1		(6.6)	4.6:	4.0	75	1.28	0.22	0.50	−3.5
			A4 IV	1.6		(4.5)		6.6			0.32	0.26	−1.1
AG Per	d	2.03	B4 (V)	5.2	3.7	(3.0)	3.4	3.6	91	0.99	0.26	0.39	−2.7
			B5 (V)	4.6	3.4	(2.8)	3.2	3.3	72:	0.85	0.24	0.37	−2.2
SX Aur	sd	1.21	B3 V	11.2		5.2:		4.0	243	1.12	0.42	0.44	−3.8
			B3 V	5.9		4.3:		4.0			0.35	0.32	−3.3
HD 47129	sd	14.40	O8 V	∼ 51	13.2			12.3	150	3.23	0.11	0.36	−8.5
			O8 (F)	∼ 64					127			0.40	
V Pup	sd	1.45	B1 V	18		6.1:		7.6	185	0.87	0.37	0.43	−5.1
			B3 (IV)	10		5.3:		5.8			0.32	0.33	−3.8
α Vir	d	4.01	B1.5 IV-V	10.9		8.1	6.5	7.2	170	1.66	0.29	0.42	−5.4
			B3 V	6.8		3.7:		4.0	115	2.28	0.14	0.34	−3.0
μ^1 Sco	sd	1.45	B1.5 V	14	5.1	5.2		6.2	252	1.42	0.33	0.42	−4.5
			B6 (III)	9	6.1	5.8		5.4			0.40	0.34	−3.2
U Oph	d	1.68	B4 V	5.0		3.4	3.5:	3.6	107	1.05	0.27	0.39	−2.6
			B5 V	4.5		3.1	3.3:	3.3	87	0.93	0.25	0.37	−2.0
u Her	sd	2.05	B1.5: V	7.9		(4.5)	5.5	6.2	119	0.88	0.37	0.47	−4.7
			B5 (IV)	2.8		(4.3)	4.9:	4.8	90:	0.74	0.33	0.29	−3.0
V356 Sgr	sd	8.90	B3 V	12.1		4.9		4.0	350	12.6	0.11	0.46	−3.6
			A2 II	4.7		11.0		14.3	90	1.44	0.24	0.30	−2.4
Z Vul	sd	2.45	B4 V	5.4		4.7		3.6	155	1.60	0.31	0.45	−3.3
			A2-3 III	2.3		4.7		4.7			0.31	0.31	−0.5
σ Aql	d	1.95	B3 V	6.8		(4.2)	4.3	4.0	123	1.10	0.28	0.40	−3.3
			B3 V	5.4		(3.3)	3.8	4.0	142	1.44	0.25	0.36	−3.1
V448 Cyg	sd	6.52	B1 *Ib*-II	17.5	13.3	16.5:		17.1	173	1.68	0.27	0.36	−6.8
			O9.5 V	22.4	10.2	7.8:		10.1			0.20	0.40	−7.6
V453 Cyg	d	3.88	B0.5 IV	17.8	8.2	(7.5)		11.1	266	2.49	0.25	0.40	−6.4
			B0.5 IV	13.7	6.5	(6.2)		11.1			0.20	0.36	−5.9
Y Cyg	d	3.00	B0 IV	17.5		5.9	5.2	11.4	145	1.46	0.21	0.38	−6.3
			B0 IV	17.5		5.9	5.2	11.4	140	1.41	0.21	0.38	−6.3
AH Cep	d	1.77	B0.5 IV	16.1		(6.0)	7.0	11.1	210	1.05	0.37	0.39	−6.1
			B0.5 IV	13.9		(5.4)	6.5	11.1	195	1.05	0.34	0.37	−5.9
CW Cep	d	2.73	B1.5 V	10.0	6.7	(5.8)		6.2	132	1.06	0.30	0.38	−5.1
			B1.5 V	9.8	5.8	(4.4)		6.2	138	1.28	0.26	0.38	−4.8

Evidence exists that the less massive components of V356 Sagittarii (Plavec 1967) and of V448 Cygni (Sahade 1962) either fill, or did recently fill, their Roche lobes, and these systems are here designated "sd". SX Aurigae, V Puppis, and μ^1 Scorpii have very short orbital periods and are nearly contact systems. The system types of AO Cassiopeiae and HD 47129 are not entirely clear.

Column (3): orbital period.

Column (4): spectral type and luminosity class, taken from Stothers's (1972) tabulation or else estimated from published descriptions of the spectrum.

Column (5): mass, taken from Stothers's (1972) tabulation.

Column (6): radius, derived from the Stefan-Boltzmann law (for the members of clusters). Absolute magnitudes are adopted from Stothers (1972), while effective temperatures and bolometric corrections are adopted from Morton (1969) for O5–B0.5 stars and from Morton and Adams (1968) for B1–A4 stars. Morton's effective-temperature scale may be too cool (by < 10%) in the range O5–B0 (Auer and Mihalas 1972; Conti 1973).

Column (7): radius, derived from the orbit solution. Reliable stellar radii of this kind are listed by Harris, Strand, and Worley (1963) for several of our systems, and are here supplemented by radii for α Virginis (Herbison-Evans et al. 1971), AO Cas and V448 Cyg (Sahade 1962), and SX Aur and V Pup (Popper 1943). Radii for the remaining systems (Plaut 1950; Plavec 1967; Kriz 1969) are more uncertain, as indicated by the parentheses, and will not be used in what follows.

Column (8): radius, derived from the spectroscopic surface gravity combined with the mass from the orbit solution. For each star the mean of two surface gravities determined by Olson (1968*a*) on the basis of two different line-broadening theories has been adopted, in view of the persisting uncertainty of the various theories (Dufton 1972). Watson (1972) has determined the surface gravities for the components of α Vir on the basis of the ESW line-broadening theory.

Column (9): radius, derived from the Stefan-Boltzmann law by using the statistical calibration of absolute magnitudes as a function of MK spectral classification (Blaauw 1963) and Morton's effective temperatures and bolometric corrections as above. An improvement might be to use estimates of individual absolute magnitudes published by Koch, Olson, and Yoss (1965), Olson (1968*a*), and McNamara (1966), but most of these measurements refer to the *mean* of the two components.

Column (10): rotational velocity, corrected for orbital inclination by assuming parallel axes of rotation and orbital revolution. Sources of $v \sin i$ are given by Stothers (1972), who, however, inadvertently listed v in his Table 4 for stars measured by Koch et al. (1965) and by Olson (1968*b*). Rachkovskaya (1971) and Watson (1972) have measured $v \sin i$ for the components of CW Cephei and α Vir, respectively. Orbital inclinations are adopted from Batten (1967), with the exception of those for HD 47129 (Sahade 1962) and α Vir (Herbison-Evans et al. 1971).

Column (11): ratio of observed rotational velocity to the "synchronous" rotational velocity, where $v_{\rm syn} = 2\pi R/P$ (P is orbital period). We have adopted as the "best" radius for each star the first one listed in columns (6)–(9), ignoring radii enclosed in parentheses.

Column (12): ratio of the "best" radius to the orbital separation, where the latter quantity is derived from the adopted P and $\mathfrak{M}_A + \mathfrak{M}_B$ by Kepler's law.

Column (13): ratio of the radius of the Roche lobe to the orbital separation.

Column (14): bolometric absolute magnitude, derived from the effective temperature and the "best" radius.

The accuracy of the "best" radius for any star is usually found to be not much greater, on the average, than that of the other measured radii (with the exception of the uncertain statistical radius), whose typical errors are ~15%. Our present data for radii suggest that all of the *detached* components with spectroscopic luminosity classes of III and IV actually belong to luminosity class V. However, these components lie in the difficult spectral range O9–B0.5, and, in fact, luminosity class V has sometimes been assigned to them: AO Cas (Roman 1956; Olson 1968*a*), V453 Cygni (Roman 1951; Guetter 1968), Y Cygni (Roman 1956; Olson 1968*a*), and AH Cephei (Morgan, Code, and

Whitford 1955; Olson 1968*a*). The more massive component of Z Vulpeculae also has a discrepant statistical radius, but here a spectral type of B3 (Popper (1957) gives B3–B5) would remove most of the discrepancy.

Since the error in effective temperature due to the discrete spectral classification and to the imprecise temperature scale is probably $\sim$10%, the total error in the derived bolometric absolute magnitudes will be about 0^m5. For cluster members, the likely errors in M_v (Blaauw 1963) and in B.C. (Bradley and Morton 1969) produce the same total error in M_{bol}. An intercomparison of mass determinations and their errors (Plavec 1967; Popov 1968; Kriz 1969) suggests that the masses may have an error of $\sim$10%. Because the accuracy of measuring $v \sin i$ is $\sim$15% (Koch et al. 1965; Slettebak 1970), the typical error in v/v_{syn} is likely to be $\sim$20%, which seems to be corroborated by the fact that no v/v_{syn} for our stars is formally found to be less than 0.8.

Altogether, we have the following estimated errors: M_{bol} ($\pm$0.5), Sp ($\pm$1), $\log T_e$ ($\pm$0.04), $\log R$ ($\pm$0.06), $\log \mathfrak{M}$($\pm$0.04), and $\log v/v_{syn}$ ($\pm$0.08).

III. General Rotational Properties

By assuming that the axis of rotation is always parallel to the axis of orbital revolution, we find $\langle v \rangle = 165$ km sec^{-1} for the 24 O–B4 main-sequence stars in our sample. The observed value of $\langle v \sin i \rangle$ for (mostly) single O–B4 main-sequence stars is about 160 km sec^{-1} (Slettebak 1970). But since the rotational axes of these stars are probably randomly oriented in space (Kraft 1970), we find $\langle v \rangle = (4/\pi) \langle v \sin i \rangle =$ 200 km sec^{-1}, which is significantly larger than the value for binary members. The difference is usually presumed to be due to the tidal coupling of axial rotation to orbital revolution in close binary systems.

Two pieces of observational evidence support the basic assumption that the axes of rotation and of orbital revolution are at least approximately parallel. First is a weak correlation observed between $v \sin i$ and spectral type, as well as the absence of very large and of very small values of $v \sin i$ (Koch et al. 1965). Second is the approximate synchronism that emerges on this assumption between axial rotation and orbital revolution (Plaut 1959; Koch et al. 1965; Olson 1968*b*; Plavec 1970; van den Heuvel 1970; Nariai 1971; Rachkovskaya 1971).

Limitations on the degree of synchronism attained are best seen in a plot of v/v_{syn} against P, or against R/a which is more meaningful physically (Olson 1968*b*; Plavec 1970). In Figure 1, which shows such a plot, we find that significantly faster-than-synchronous rotation occurs only when the tidal force is relative weak, i.e., when $R/a < 0.3$ (or $P > 2$ days). However, this diagram is somewhat misleading because the nonsynchronous stars belonging to the *detached* systems (we may also include AR Cassiopeiae and α Coronae Borealis) occur exclusively in systems with large orbital eccentricities. In fact, we find $e > 0.05$ only if $P > 2$ days. For detached systems having negligible orbital eccentricity, the data of Olson and Plavec indicate that synchronism occurs out to *at least* $R/a =$ 0.13 (or $P = 4$ days). The slow tidal evolution of these systems has been discussed by Kopal (1972). The break in Figure 1 near $R/a = 0.3$ for the detached components of *semidetached* systems (we may also include U Cephei and RS Vulpeculae) is not due to a change from small to large orbital eccentricities, because all of the semidetached systems (except for λ Tauri) have nearly circular orbits. The evolution of the semidetached systems will be discussed in sections V and VI.

Further progress in determining the *internal* state of rotational motions in massive stars depends on a study of the (mass, luminosity), (mass, spectral type), and (mass, radius) planes, which are shown in Figures 2, 3, and 4. In each figure, the theoretical main-sequence band for nonrotating hydrogen-burning stars (Stothers 1972; Ezer and Cameron 1967) is shown for a (hydrogen, metals) content of $(X, Z) = (0.739, 0.021)$. Changes in the adopted chemical composition induce the following *approximate* changes in the location of the band over the mass range 5 to 15 $\mathfrak{M}_\odot$:

$$\Delta M_{bol} = 4.5\,\Delta X + 10\,\Delta Z \quad , \qquad (2)$$

$$\Delta \log T_e = -0.4\,\Delta X - 2\,\Delta Z \quad , \qquad (3)$$

$$\Delta \log R = -0.1\,\Delta X + 2\,\Delta Z \quad . \qquad (4)$$

Therefore the band as plotted should represent nonrotating Population I stars very closely, since their most probable initial chemical composition

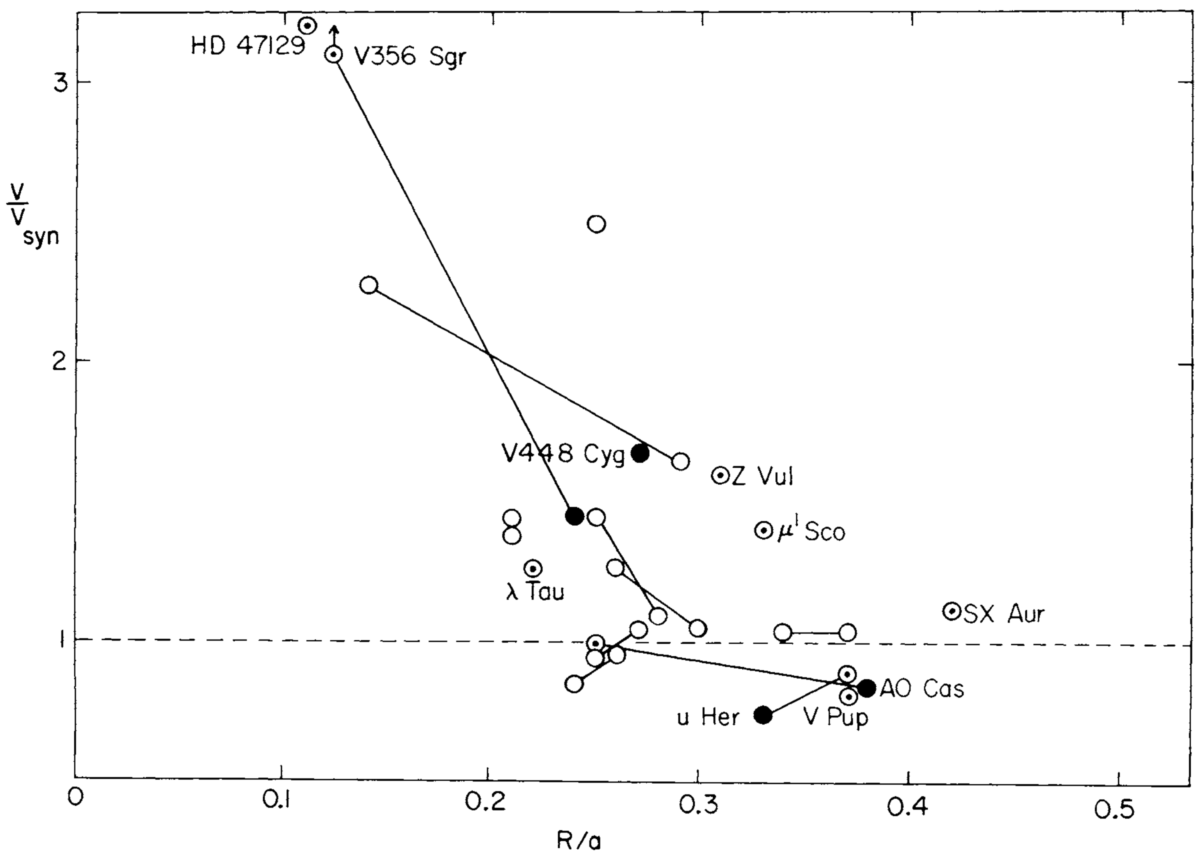

FIG. 1 — The ratio of the observed equatorial velocity of rotation to the velocity expected for synchronism with the orbital revolution is plotted against the ratio of the observed stellar radius to the orbital separation, for the components of massive close binary systems. The circles refer to the following components: *open*, component of a detached system; *dotted*, detached component of a semidetached system; *filled*, contact component of a semidetached system. Unbroken straight lines connect components of the same system.

is $X = 0.70 \pm 0.03$ and $Z = 0.03 \pm 0.01$ (Stothers 1973). The theoretical locus for nonrating homogeneous helium-burning stars (Divine 1965) is also shown in Figure 2; it is relatively insensitive to Z.

IV. Detached Systems

Virtually all of the components of detached systems are situated well within the main-sequence band of Figures 2, 3, and 4. The small scatter above the ZAMS line can be attributed to the effects of partial evolution and to the observational errors. The apparent youthfulness is confirmed by the fact that three of the systems are known members of clusters or associations (Stothers 1972) and have components that lie definitely below the top of the main sequence in the cluster H-R diagrams.

It is difficult to verify the predictions of rotation theory in detail. Uniform rotation is expected to change the luminosity very little (only 0^m1 at critical rotation for breakup) and to reduce the effective temperature approximately as follows:

$$\delta \log T_e = 0.065\,\alpha \quad , \tag{5}$$

where α is the ratio of centrifugal force to gravity at the surface of the unperturbed star viewed equator-on (Sweet and Roy 1953). More recent models agree with this prediction to within several percent, for $\alpha < 0.2$ (Faulkner, Roxburgh, and Strittmatter 1968; Kippenhahn, Meyer-Hofmeister, and Thomas 1970; Sackmann and Anand 1970). Moreover, tidal distortion due to a stellar companion is found to be negligible in comparison with the rotational effect (Jackson 1970; Kippenhahn and Thomas 1970). Since the fastest rotator in our sample of stars has $\alpha \approx 0.2$,

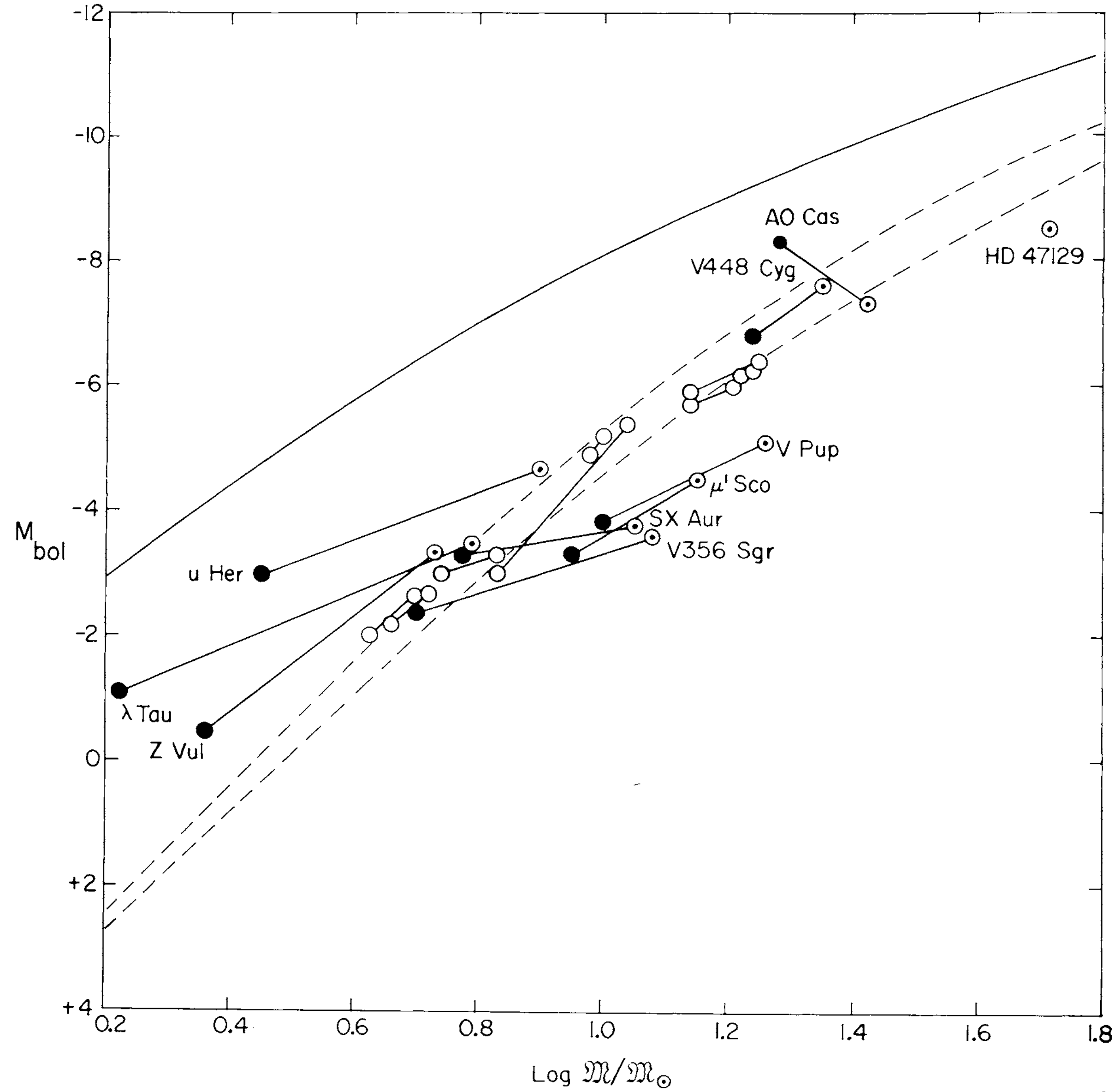

FIG. 2 — (Mass, luminosity) — diagram. The meaning of the symbols is the same as in Figure 1. The lower and upper dashed lines refer to the theoretical nonrotating ZAMS (zero-age main sequence) and TAMS (terminal-age main sequence), respectively, for normal hydrogen-burning stars. The continuous curved line refers to the theoretical locus of homogeneous helium-burning stars.

we find $\delta \log T_e \approx 0.01$; this shift, unfortunately, is too small to be detected within the observational error of ± 0.04. Even if our assumption of parallel axes of rotation and of revolution is badly off, α could at most be unity, for which $\delta \log T_e \approx 0.02$ (Sackmann and Anand 1970).

Strongly nonuniform rotation, with the angular velocity increasing steeply toward the stellar center, yields a much larger decrease of luminosity and of effective temperature for the same observed equatorial velocity at the surface (Mark 1968; Bodenheimer and Ostriker 1970; Bodenheimer 1971). Inspection of Figures 2 and 3 shows, however, that the members of detached systems seem to be in uniform rotation, to within the uncertainty of the data. Thus the rotational angular momentum J_{unif} of each system is calculated to be less than 1% of its total

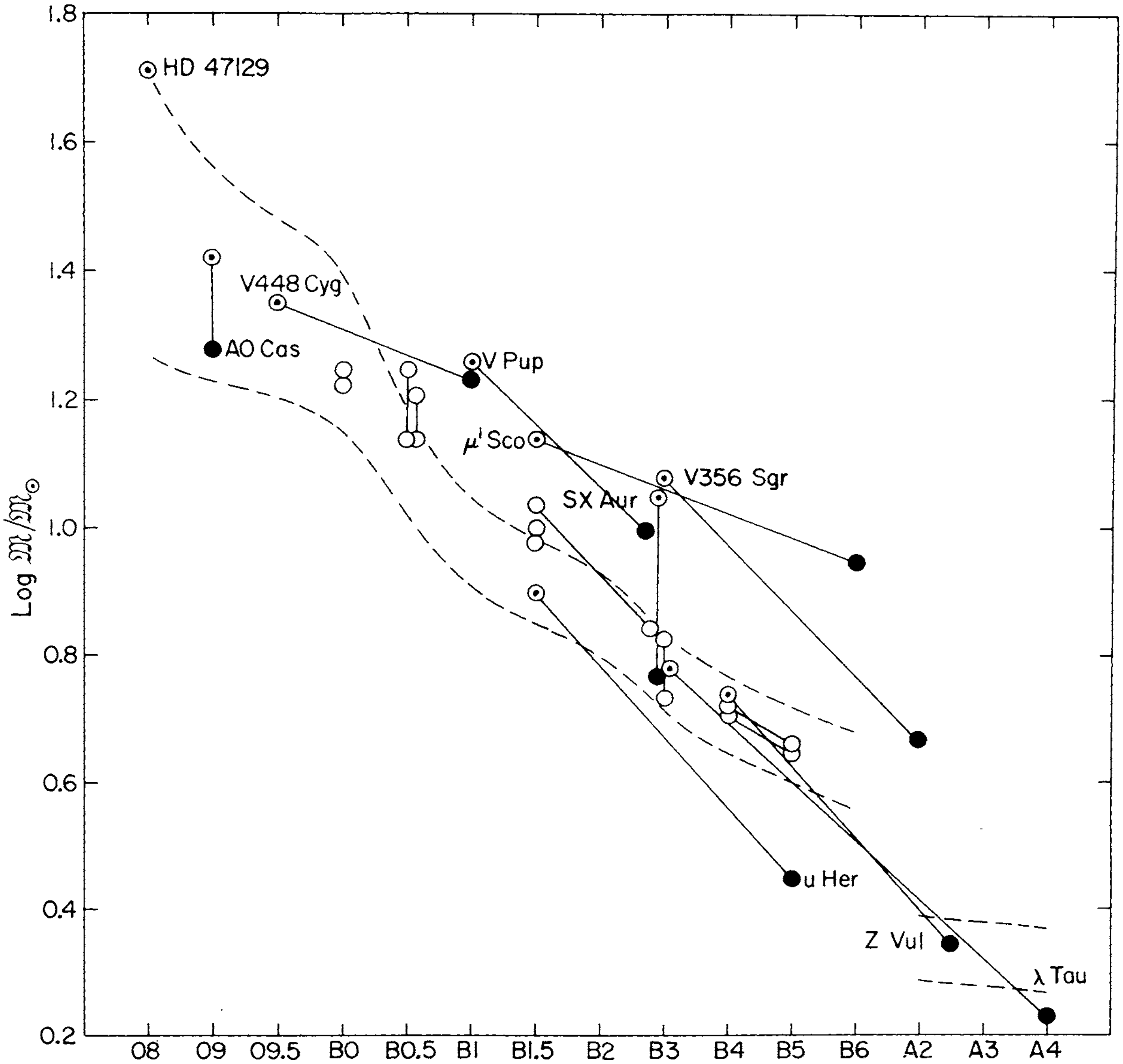

FIG. 3 — (Mass, spectral type) — diagram. The meaning of the symbols and lines is the same as in Figure 2. The scale of spectral types is broken between B6 and A2.

(orbital plus rotational) angular momentum, as found by evaluating

$$J_{\mathrm{unif}} = (2/3) v R \mathfrak{M} I \quad , \qquad (6)$$

where v is the equatorial rotational velocity at the surface and $I \approx 0.10$ (section VI). From the apsidal motion observations of Y Cyg and AG Persei, Kopal (1972) has derived the same small percentage.

Uniform rotation (or a fair approximation thereof) seems also to characterize single stars on the upper main sequence (Stothers 1973). However, noticeable nonuniformity of rotation must set in just after the main-sequence phase, possibly as a result of the establishment of the hydrogen-burning shell between the contracting core and the expanding envelope. The reason is that supergiants which are still burning core hydrogen always have spectral types earlier than B1.5 (Stothers 1972), and this spectral type is found to sharply divide swiftly rotating supergiants from very slowly rotating ones (Boyarchuk and Kopylov 1958). The supergiants in binary systems (Stothers and Lloyd Evans 1970) seem also to conform to this division.

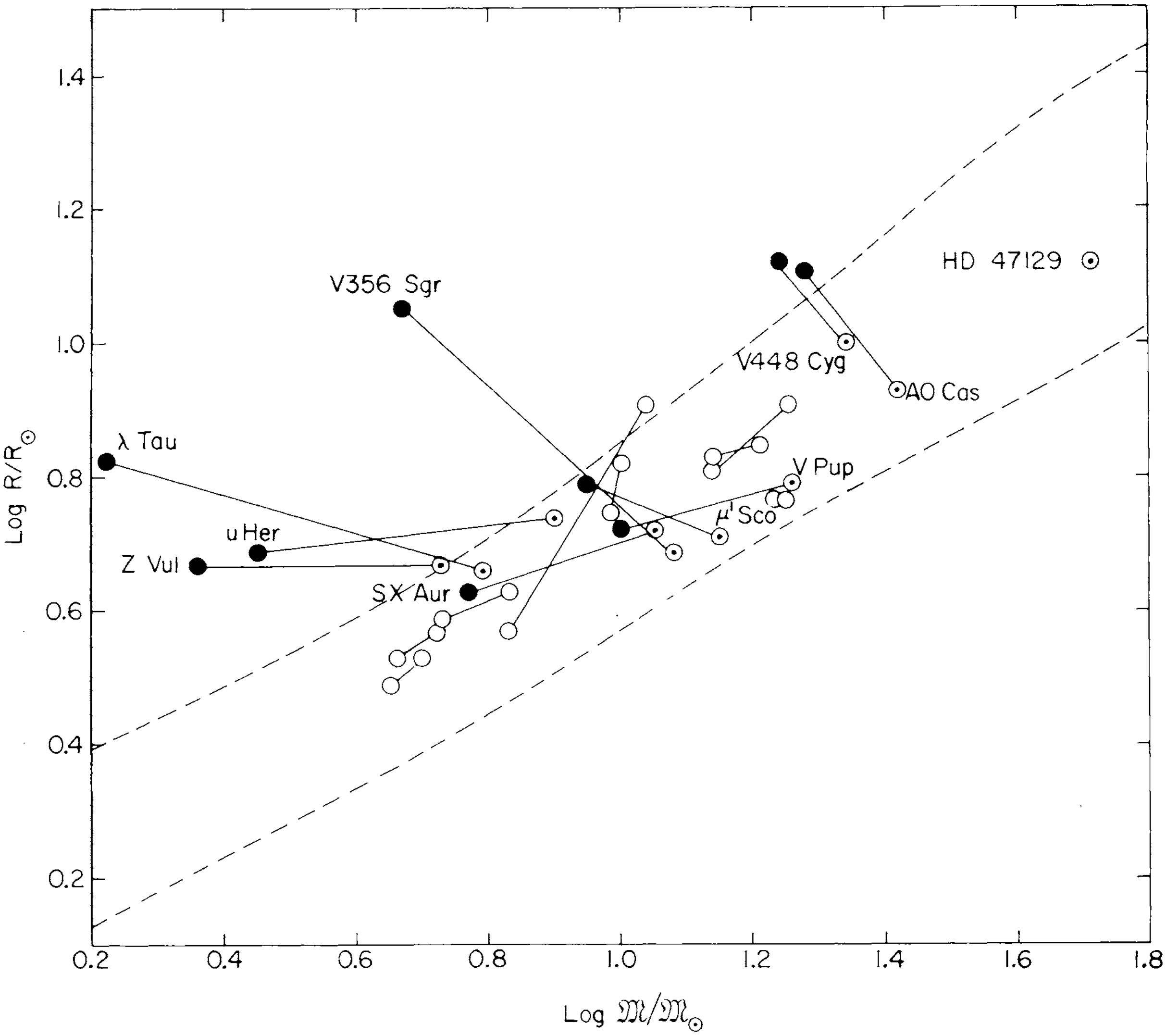

FIG. 4 — (Mass, radius) — diagram. The meaning of the symbols and lines is the same as in Figure 2.

V. Evolution in Cases A and B

In order to interpret the observations of the semidetached systems, it is necessary to put together briefly a composite theoretical picture of evolution in massive close-binary systems (for a complete set of references, see Paczynski 1971).

For the moment, we ignore the obscure pre-main-sequence history of the system and begin with the evolution of the components on the main sequence. The primary star (being the initially more massive component) evolves first, expanding its radius until it reaches its Roche lobe. Thereupon matter streams off the surface of the primary at an increasingly rapid rate (Helmholtz-Kelvin time scale) through the vicinity of the inner Lagragian point, and either strikes the secondary directly or forms around it a rapidly rotating ring, disk, or envelope, which is subsequently accreted by the central star. During the most rapid stages, the luminosity of the primary may become temporarily depressed below the equilibrium value for its instantaneous mass. Eventually a slower phase of mass exchange ensues, during which the original primary continues to fill its Roche lobe and appears as a cool subgiant, greatly overluminous for its mass (because it still possesses its whole helium-rich core). It is expected to be rotating in synchronism, or in slightly less than synchronism, with the orbital motion.

At this point two cases must be differentiated. If the primary initially began to lose matter before hydrogen was exhausted at the center (case A), the slow phase of mass loss proceeds on a nuclear (hydrogen-burning) time scale in the subgiant configuration. As hydrogen is further depleted, the luminosity and radius continue to rise. If, on the other hand, the primary began to lose matter during the core-contraction phase following central hydrogen exhaustion (case B), the slow phase of mass transfer is much more efficient, but more short-lived, being terminated by helium ignition at the center of the primary. Then the primary, having been stripped practically down to its helium core, contracts on a gravitational time scale toward the helium main sequence where it appears as a luminous hot subdwarf. It will be rotating very fast if it has conserved angular momentum during the contraction phase. In both case A and case B, the subsequent evolution of the system depends crucially on what has happened to the secondary.

The history of the secondary hinges on the validity of the standard assumption of conservative mass exchange, i.e., the conservation of total mass and total orbital angular momentum. With this assumption, the mass ratio of the components is always found to be more than reversed (except in extreme examples of case B), and the orbital period and separation are increased, after a momentary decrease at the beginning of the rapid phase. However, two sinks of orbital angular momentum must be considered. First is the angular momentum picked up by the secondary as rotational angular momentum during the process of mass accretion. Regardless of how rapidly this angular momentum is redistributed throughout the interior of the secondary, the turbulent surface layers, at least, should be rapidly synchronized with the orbital revolution by the tidal forces, if the separation of the components is small. The second sink of orbital angular momentum is the angular momentum carried away by mass ejected from the system as a whole. Loss of orbital angular momentum will reduce the orbital period and separation, unless the ratio of ejected mass to angular momentum is excessively large.

Although a small fraction of all semidetached systems (or of systems with undersize subgiants) may be in the pre-main-sequence phase of evolution, systems in this phase are more likely to be discovered already detached, because the evolutionary time scale is relatively longer at smaller stellar radii near the ZAMS. In fact, the substantial evidence for heavy mass exchange in semidetached systems virtually proves that they are evolved systems (Crawford 1955; Piotrowski 1964; Huang 1966; Paczynski 1966, 1967*a*, 1971; Zahn 1966; Hall 1967, 1968; Paczynski and Ziolkowski 1967; Plavec 1968, 1973; Ziolkowski 1969; Cisneros-Parra 1970). This conclusion is corroborated by the observation that the massive components of three semidetached systems which are known members of clusters and associations (Stothers 1972) lie definitely on the main-sequence turnups in the H-R diagram, and have masses characteristic of evolved stars in these stellar groups.

Among the massive systems of Table I, case A can explain the properties of the semidetached systems far better than can case B. The specific reasons are listed here since some of these reasons seem not to have been advanced before. First, case B ought to produce very few semidetached systems because the semidetached phase in case B is expected to be very short lived (Helmholtz-Kelvin time scale). Second, the slowest rate of change of orbital period predicted by the models for case B is roughly 10^{-8} (in dimensionless units), which is one to two orders of magnitude faster than the changes actually observed (Wood and Forbes 1963). Third, the final orbital period after rapid mass exchange is predicted to be, typically, > 10 days for case B and < 10 days for case A; all the observed systems have $P < 10$ days. Fourth, a very large final mass ratio (typically > 5) is predicted for case B as compared with case A, but the largest mass ratio actually observed is only 3.8. Fifth, in case B, the typical luminosity of the contact component should be close to that for a pure helium star of the same mass; this is not observed (Fig. 2). Sixth, the radius and luminosity class of the contact component are expected to correspond to at least a bright (class II) giant, which, with the exception of V356 Sgr and V448 Cyg, is not found to be the case. Seventh, a very large overabundance of helium and of nitrogen is predicted to be visible at the surface of the contact component (and, to a much lesser extent, of the detached component) for case B, but, to the best of our knowledge, such a large overabundance has not been detected (see Olson 1968*a*).

We must emphasize that the second, third, and fourth arguments are critically dependent on the assumption of *conservative* mass exchange between the components. Nonconservative effects, which are observationally very likely (Paczynski and Ziolkowski 1967; Ziolkowski 1969; Plavec 1973), would probably reduce the final orbital period as well as the final mass ratio, and therefore would probably draw relevant models for case B closer to the observed stars; but conservative mass exchange for case B with extreme initial conditions can also achieve the same effect (Paczynski 1967*b*). However, the first and fifth arguments alone confirm that the semidetached systems of Table I have evolved according to case A.

A few massive candidates for case B have been proposed elsewhere (Paczynski 1967*b*; Plavec 1968, 1973). The most notable candidate is β Lyrae.

VI. Semidetached Systems

Three empirical groups of semidetached systems can be distinguished through an examination of Figures 1 to 4. For the purposes of exposition, we shall consistently refer to the detached component (the recipient of mass) as the "primary" and to the contact component (the donor of mass) as the "secondary".

Group I (μ^1 Sco, V Pup). The primary is a main-sequence star, underluminous and cool for its mass, and the secondary is a "contact" subgiant or giant, in a similar physical state. The orbital period is very short (~1.5 days). Surface rotation seems to be synchronized well with orbital revolution. SX Aur may belong to this group, although the secondary component looks almost like a normal dwarf.

Group II (V356 Sgr). The primary is a main-sequence star, underluminous and cool for its mass, and the secondary is a "contact" subgiant or giant, of approximately normal luminosity but cool surface temperature. The orbital period is relatively long (~10 days). The contact component corotates with the system, while the detached primary rotates much faster than synchronously. Probably HD 47129 and β Lyr belong to this group or to group I.

Group III (Z Vul, λ Tau, u Herculis). The primary appears to be a bright main-sequence star, and the secondary is a "contact" subgiant or giant, overluminous and overly hot (or else normally hot) for its mass. The orbital period is moderately short (~3 days). Both components corotate with the system. To this group probably belongs AO Cas. V448 Cyg may represent a transition case between groups II and III.

It will be convenient, first, to consider together for each group the secondary component and the system as a whole, and later to discuss the primary component. Group I systems are apparently found in the rapid phase of mass transfer. This is suggested by the short orbital periods, the moderate mass ratios, and the underluminosities of the mass-losing components. However, theory predicts that the duration of the secondary's underluminous stage is less than $10^{-3}\tau_H$ where τ_H is the total lifetime of core hydrogen burning, and that the duration of the rapid phase as a whole is only $10^{-2}\tau_H$. For very close systems like those in group I, the rapid accretion of mass would also be expected to brighten and expand the primary considerably, so that a contact system is temporarily formed (Benson 1970), but probably only SX Aur among our systems could be a contact system. Moreover, the predicted rate of orbital period change during the secondary's underluminous stage is 10^{-5} (in dimensionless units), which is 4 to 5 orders of magnitude larger than the upper limits on the rates of change actually observed (Hogg 1946; Stibbs 1948; Wood and Forbes 1963). Of course, nonconservative mass exchange could drastically reduce the expected rates of period change.

Therefore the only cogent argument in favor of very rapid mass transfer in group I systems is the secondary's underluminosity. The secondary of SX Aur, however, is not underluminous. The secondaries of μ^1 Sco and V Pup would also have normal luminosities if their masses were revised downward by 20%, their radii downward by 50%, or their spectral types from B6 to B3 (for μ^1 Sco) and from B3 to B1.5 (for V Pup). For such close systems with tidally distorted components of similar spectral type, the large errors implied are not impossible, except that the luminosity of μ^1 Sco is independently known from a cluster distance modulus. The origin of the 1-magnitude underluminosities observed for the secondaries remains a mystery.

Group II systems are very similar to those of group I, except for the absence of underluminosity in the secondary and the greater orbital separation, which weakens the effect of tides on the rotation of the mass-gaining primary. These systems must be in the slow phase of mass transfer. β Lyr, whose rate of orbital period change is 3×10^{-7} (Wood and Forbes 1963), is probably just entering the slow phase, and its mass-losing component seems to be rotating nearly synchronously, while the mass-gaining component is rotating near breakup (Huang 1966).

The systems of group III have mass-losing components that are unusually luminous, presumably as a result of being more evolved than their counterparts in groups I and II. Their effective temperatures are high for their masses, but otherwise low from the point of view of their location in the H-R diagram. Since these systems are definitely in the slow phase of mass transfer, it is worth noting that their observed rates of orbital period change are undetectably small (Wood and Forbes 1963), just as is expected theoretically. The difference of orbital period between groups II and III is probably due to a difference of central hydrogen content in the mass-losing component when the transfer of mass began, rather than to a subsequent decrease of orbital separation. However, even though very little mass is transferred from the contact component during the slow phase, the transfer of angular momentum is large, and the loss of most of this material from the system as a whole (which is easier at this stage because the gravity is weaker) might significantly reduce the orbital period. On the other hand rotational spin-down of the detached component will transfer angular momentum back to the orbit and will tend to increase the orbital period again. Evidence discussed below suggests that the latter effect is probably important in explaining the difference in orbital periods between groups I and III, and so we prefer the first-mentioned explanation for the difference between groups II and III.

It has been seen that, in terms of the secondary component and the system as a whole, groups I, II, and III represent in some sense an evolutionary progression. If so, the mass-gaining component must evolve as follows. During the rapid phase it becomes underluminous and cool with respect to a ZAMS star of the same mass, but gradually it evolves into a normal main-sequence star, and then brightens up. The key to a proper understanding of this sequence seems to be the primary's underluminosity, which can arise either if the originally low-mass, and hence low-luminosity, mass-gaining star accreted very slowly the massive disk of transferred material (which would probably appear rather cool) or if the mass-gaining star accreted the disk very rapidly and absorbed an appreciable amount of angular momentum (which would reduce the luminosity and effective temperature). The recovery to a normal main-sequence state would proceed, respectively, by gradual completion of the accretion process or by rotational spin-down induced by the tidal force of the companion. In both cases, the last stage of evolutionary brightening would proceed in a consolidated star undergoing normal hydrogen depletion in its core. Figure 4 confirms that the radius of the star in this last stage is significantly larger than its ZAMS radius; thus the star cannot be evolving homogeneously, as would be the case if its radius had been found to be of nearly ZAMS size (cf. Roy 1952). In the "normalized" H-R diagram of Figure 5, where the origin is taken to be the ZAMS state (for each stellar mass), each of the bright primaries is found to lie close to the evolutionary track for a nonrotating, or slowly rotating, main-sequence star. Therefore the effect on the primary of the continuing slow mass transfer from the secondary must be slight.

Two lines of argument support the rotational explanation of the primary's underluminosity as opposed to the slow-accretion explanation. First, the shape of the "star" would be flat or ringlike in the latter situation, while, in the former, its shape would be oblate-spheroidal (for uniform rotation, which is not likely here) or toroidal (for strongly nonuniform rotation). With the possible exception of β Lyr, which, after all, is probably at the end of the rapid phase, there seems to be no observational evidence for *very massive* disks in the systems considered here. Moreover, the surface rotational velocities and under-

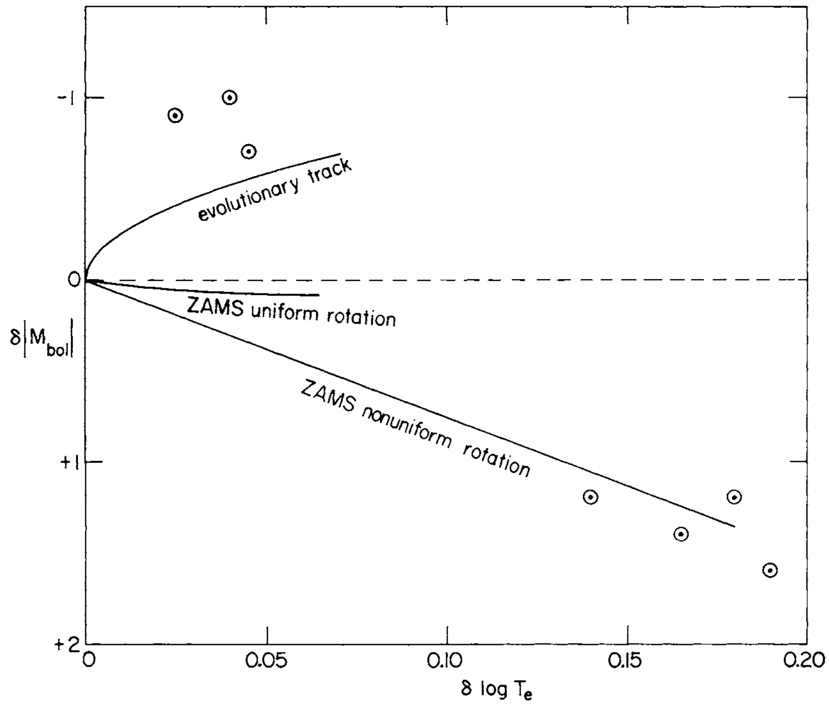

FIG. 5 — Underluminosity of a star with respect to a nonrotating ZAMS star of the same mass is plotted against the corresponding reduction of effective temperature, for the detached components of semidetached systems. Also shown are: the evolutionary track for a nonrotating, or slowly rotating, star; the shift for a ZAMS star in uniform rotation; and the shift for a ZAMS star in nonuniform rotation (the shifts refer to Bodenheimer's angular momentum distributions D and A, respectively). The three lines plotted are relatively insensitive to stellar mass.

luminosities of the primaries of these systems are not so very extreme that it would be easy to detect toroidal distortion of the "ellipsoidal" shape actually observed for these objects (Popper 1943, 1955; Hogg 1946; Stibbs 1948), but a modern attempt should be made.

The second line of argument in favor of a rotational explanation is the observed progression of surface rotational velocities. However, the argument is clouded somewhat by the different time scales operating. Zahn (1966) finds that the tidal force on a radiative envelope is only effective on a time scale much longer than the nuclear lifetime of the star, even in a nearly contact system. But he finds that the surface tides may induce a small surface convection zone, whose rotation could then become synchronized with the orbital revolution extremely quickly. Neither of these time scales seems to apply to our observed systems but an intermediate time scale does, and this may support Zahn's ideas to some extent. Nevertheless, his results, as they stand, cannot be used here.

Instead, we shall proceed by adopting a phenomenological description. In an *isolated* rotating star, the Eddington-Sweet circulation time is given approximately by (Sweet 1950)

$$\tau_{\rm rot} \sim \tau_{\rm HK}/\alpha \quad , \tag{7}$$

where $\alpha = Rv^2/G\mathfrak{M}$, the ratio of centrifugal force to gravity at the equator, and

$$\tau_{\rm HK} = G\mathfrak{M}^2/RL \quad , \tag{8}$$

the Helmholtz-Kelvin gravitational time scale. In terms of the nuclear time scale for core hydrogen burning,

$$\tau_{\rm HK} \sim 10^{-2}\,\tau_{\rm H} \quad . \tag{9}$$

By analogy with Sweet's result, we assume that the time scale to establish synchronization of rotation in the envelope of star A in the tidal force field of companion B is

$$\tau_{\rm syn} \sim \tau_{\rm HK}/C\beta^n \quad , \tag{10}$$

where $\beta = (\mathfrak{M}_{\rm B}/\mathfrak{M}_{\rm A})(R_{\rm A}/a)^3$, the ratio of distortion force to gravity at the equator of star A, and C is a constant.

The semidetached phase of evolution in a close binary system has been computed to last

$$\tau_{\rm sd} = \gamma\,\tau_{\rm H} \quad , \tag{11}$$

where $\gamma \sim 1$ for case A and $\gamma \sim 10^{-2}$ for case B. According to our admittedly slender statistics, synchronous rotation of the envelope of the primary is not uncommon among semidetached systems; in any case, we require that

$$\tau_{syn} < \tau_{sd} \quad . \tag{12}$$

This leads to an observable quantity,

$$\frac{R_A}{a} \sim \left(\frac{10^{-2}}{\gamma C} \right)^{1/3n} \left(\frac{\mathfrak{M}_A}{\mathfrak{M}_B} \right)^{1/3} , \tag{13}$$

which represents the smallest value of R_A/a for which synchronism is likely to be observed in a random sample of semidetached systems. Consider case A with $\gamma \sim 1$. A straightforward guess for n would be $n = 1$, but Zahn's results suggest that $n = 2$ since his tidal scales are proportional to P^4 (i.e., to a^6). We then find the following results for $C = 1$ and for mass ratios $\mathfrak{M}_A/\mathfrak{M}_B$ in the range from 1 to 3. For $n = 1$, $R_A/a = 0.2$–0.3; and, for $n = 2$, $R_A/a = 0.5$–0.7. Dziembowski's (1967) particular solution for τ_{syn} gave $n = 2$ and $C \sim 75$; this yields $R_A/a = 0.2$–0.3. Considering the necessary crudeness of our approach, we obtain quite satisfactory agreement with the observational results for the primaries of semidetached systems in Figure 1.

Rotation of the convective core, which affects the luminous output of the star, is more problematical. Zahn's time estimates are quite uncertain here, but they are extremely long for the large injections of angular momentum into the core implied by the observed underluminosities in Figure 5 (see p. 374). Since the continual accretion of matter by the primary during the slow phase of mass transfer will keep the star stirred up to some extent (but not completely, in view of the evidence for later inhomogeneous evolution), we can probably expect a somewhat shorter spin-down time than what Zahn estimated. The present evidence of Figure 5 suggests that underluminosity of the primary is fairly common among semidetached systems (at least among the more massive, hence younger ones), so that the spin-down time can be reasonably inferred to be $\sim\tau_H$ (which is 10^7 years at $10\,\mathfrak{M}_\odot$) for $P \sim 2$ days but probably much longer for $P \sim 10$ days, in rough qualitative agreement with Zahn, who found that the spin-down time goes like P to a high (fourth) power. Thus the large underluminosities, large rotational velocities, and *long* orbital periods of the mass-gaining components in the group II systems could have grave consequences for the future interior evolution of these components.

A quantitative study of the role of the mass-gaining component in the evolution of the system as a whole can now be made on the hypothesis that each primary is rotating differentially, regardless of the magnitude of the observed surface velocity, which is far more quickly synchronized by the tidal force than is the spinning core. Bodenheimer (1971) has shown that the amount of underluminosity of a star depends only on its total rotational angular momentum, not on how this angular momentum is distributed throughout the stellar interior, although the associated reduction of effective temperature does depend on the interior distribution of angular momentum. In Figure 5, lines of increasing total angular momentum for ZAMS stars are shown for the two cases of uniform rotation and of nonuniform rotation (Bodenheimer's angular momentum distributions D and A). The underluminous primaries are seen to be quantitatively explicable by the nonuniformly rotating models.

While the tidal force of the companion causes the primary's core to spin down, the lost rotational angular momentum will go into orbital angular momentum. The future orbital periods of the systems in question can be predicted if we make the following assumptions: (1) the orbit remains nearly circular, (2) no further mass is exchanged or lost, (3) the total (orbital plus rotational) angular momentum of the system is conserved, (4) the secondary is rotating slowly (approximately synchronously) and conserves its rotational angular momentum, and (5) the final rotational state of the primary is the synchronous state. These are probably fair approximations (except for the last one in the case of group II systems, where the tidal forces are relatively weak).

The orbital angular momentum J_{orb} is given by

$$J^3_{orb} = \frac{G^2(\mathfrak{M}_A\mathfrak{M}_B)^3P}{2\pi(\mathfrak{M}_A + \mathfrak{M}_B)} \tag{14}$$

Bodenheimer's (1971) numerical data for rotating ZAMS stars can be fitted to an approximation formula giving the rotational angular momentum J_{rot} as a function of underluminosity $\delta|M_{bol}|$, as follows:

$$J_{rot} = 4.9 \times 10^{53}(\delta|M_{bol}|)^{1/2}(\mathfrak{M}/30\mathfrak{M}_\odot)^2 \text{ g cm}^2 \text{ sec}^{-1} \quad . \tag{15}$$

The particular dependence on mass is easily understood. Since, dimensionally, J_{rot} must be proportional to $\omega R^2\mathfrak{M}$ where ω is angular velocity, one finds by using the ZAMS relation

$$R/R_\odot = (\mathfrak{M}/\mathfrak{M}_\odot)^{0.55} \tag{16}$$

that J_{rot} is nearly proportional to $\mathfrak{M}^2$ for stars constructed with the same distribution of angular velocity and of mass (e.g., ZAMS stars). Bodenheimer's results were computed for models of stars of 15–60$\mathfrak{M}_\odot$ with $(X, Z) = (0.70, 0.03)$, and so are adequate for our purposes. The rotational angular momentum J_{syn} of a star spinning uniformly in synchronism with its orbital motion is

$$J_{syn} = 4\pi\mathfrak{M}R^2I/3P \tag{17}$$

where the nondimensional moment of inertia about the center I is ~0.10 for a star anywhere in the upper main-sequence band.

The change in orbital period is derived from

$$J'_{orb} + J'_{syn} = J_{orb} + J_{rot} \quad , \tag{18}$$

where primed symbols refer to the new orbital quantities, and J_{rot} and J'_{syn} are computed for the primary star only. In practice, J'_{syn} is found to be negligible in comparison to J'_{orb}; hence our neglect of possible changes in the rotational angular momentum of the secondary is justified. Predictions for the observed systems belonging to groups I and II are given in Table II. It is readily seen that the future orbital periods of group I systems are very similar to the present orbital periods of older (group III) systems! Assuming a linear rate of period increase, we predict $dP/dt \approx (P' - P)/\tau_H \sim 10^{-10}$, which is of the same order of magnitude as the upper limits on the rates actually observed. Although we have found a large ratio $\langle J_{rot}/J_{orb}\rangle = 0.21 \pm 0.05$ for the four youngest semidetached systems, confirmation of this ratio by apsidal motion observations following Kopal (1972) will be extremely difficult because the orbits are nearly circular.

A second interpretation of the orbital periods of group III systems is possible, however. Assume that mass exchange in group I systems is incomplete and that the final mass ratio will be $\mathfrak{M}_A/\mathfrak{M}_B = 3$, which is characteristic of group III systems. By ignoring the rotational angular momenta and simply equating

$$J''_{orb} = J_{orb} \quad , \tag{19}$$

final periods P'' can be derived, and are listed in Table II. Again, they are very similar to the periods of group III systems.

At the present time we cannot distinguish between the two interpretations offered, if, in fact, the orbital periods of group I and III systems are linked dynamically as an effect of interaction between the components rather than as a mere reflection of different initial conditions.

VII. Conclusion

An attempt has been made to consolidate the available observational and theoretical data concerning axial rotation of stars in massive binary systems. Some of our conclusions are not new, but fresh supporting evidence or more quantitive information has been brought to bear on those problems. Most of our results for the semidetached systems are new.

The general rotational properties of the components of massive close binary systems suggest that the axes of rotation and of revolution are parallel, and that the rotational motion of stars

TABLE II

ANGULAR MOMENTA AND FUTURE ORBITAL PERIODS OF MASSIVE SEMIDETACHED BINARY SYSTEMS

Group	System	$J_{orb} \times 10^{-53}$ (g cm^2 sec^{-1})	J_{rot}/J_{orb} (primary)	$\delta\|M_{bol}\|$ (primary)	P (days)	P' (days)	P'' (days)
I	μ^1 Sco	6.2	0.19	1.2	1.4	2.3	3.0
	V Pup	8.3	0.25	1.4	1.5	2.8	2.7
	SX Aur	3.4	0.22	1.2	1.2	2.1	2.1
II	V356 Sgr	5.7	0.18	1.6	8.9	15.2	—

in increasingly closer systems is more nearly synchronized with the orbital motion.

The detached systems are essentially unevolved, and their components are in approximately uniform rotation. Significant nonuniformity of rotation (slow surface rotation) develops later during the phase of rapid envelope expansion following hydrogen exhaustion in the core. Faster-than-synchronous rotation occurs in detached systems only when the orbital eccentricity is large.

The semidetached systems are definitely evolved, having suffered significant mass exchange between the components. In our sample, the exchange must have taken place before hydrogen exhaustion at the center of the original primary (case A). An evolutionary progression of events can be inferred from the observed states of the various systems, although the large underluminosities of the youngest mass-losing components are not understood yet. The mass-gaining component in an evolving system apparently spins up rapidly, becomes underluminous, and gradually recovers to a normal main-sequence state by virtue of the tidal effect of its companion; thereupon ordinary inhomogeneous evolution recommences in its interior. Quantitative estimates have been made of (1) the maximum orbital separation for which synchronism of surface rotation and orbital revolution can be attained in the star's lifetime, (2) the spin-down time of the stellar core, (3) the amounts of underluminosity and of reduced effective temperature due to fast interior rotation, (4) the rotational angular momentum content of the star, and (5) the future orbital period of the system.

Among the investigated semidetached systems there is some indication that the mass ratio of the two components is smaller as the total mass of the system is larger. Available models of mass exchange for case A are too few in number, particularly at very high mass, to say whether this indication may be real. In view of the rather small number of well-observed massive systems, it would be worthwhile to check the present conclusions by extending the analysis to systems of smaller mass.

REFERENCES

Auer, L. H., and Mihalas, D. 1972, *Ap. J. Suppl.* **24**, 193.

Batten, A. H. 1967, *Pub. Dominion Astrophys. Obs.* **13**, 119.

Benson, R. S. 1970, *Bull. A.A.S.* **2**, 295.

Blaauw, A. 1963, in *Basic Astronomical Data*, K. Aa. Strand, ed. (Chicago: University of Chicago Press), p. 383.

Bodenheimer, P. 1971, *Ap. J.* **167**, 153.

Bodenheimer, P., and Ostriker, J. P. 1970, *Ap. J.* **161**, 1101.

Boyarchuk, A. A., and Kopylov, I. M. 1958, *Soviet Astr.* **2**, 752.

Bradley, P. T., and Morton, D. C. 1969, *Ap. J.* **156**, 687.

Cisneros-Parra, J. U. 1970, *Astr. and Ap.* **8**, 141.

Conti, P. S. 1973, *Ap. J.* **179**, 181.

Crawford, J. A. 1955, *Ap. J.* **121**, 71.

Devinney, E. J. 1972, *Bull. A.A.S.* **4**, 269.

Divine, N. 1965, *Ap. J.* **142**, 824.

Dufton, P. L. 1972, *Astr. and Ap.* **18**, 335.

Dziembowski, W. 1967, *Comm. Obs. Roy. Belgique Uccle*, No. B17.

Ezer, D., and Cameron, A. G. W. 1967, *Canadian J. Phys.* **45**, 3429.

Faulkner, J., Roxburgh, I. W., and Strittmatter, P. A. 1968, *Ap. J.* **151**, 203.

Guetter, H. H. 1968, *Pub. A.S.P.* **80**, 197.

Hall, D. S. 1967, *A.J.* **72**, 301.

—— 1968, *Pub. A.S.P.* **80**, 477.

Harris, D. L., Strand, K. Aa., and Worley, C. E. 1963, in *Basic Astronomical Data*, K. Aa. Strand, ed. (Chicago: University of Chicago Press), p. 273.

Herbison-Evans, D., Hanbury Brown, R., Davis, J., and Allen, L. R. 1971, *M.N.R.A.S.* **151**, 161.

Hogg, A. R. 1946, *M.N.R.A.S.* **106**, 292.

Huang, S.-S. 1966, *Annual Rev. of Astr. and Astrophysics* **4**, 35.

Jackson, S. 1970, *Ap. J.* **160**, 685.

Kippenhahn, R., and Thomas, H.-C. 1970, in *Stellar Rotation*, A. Slettebak, ed. (Dordrecht: D. Reidel Publishing Co.), p. 20.

Kippenhahn, R., Meyer-Hofmeister, E., and Thomas, H.-C. 1970, *Astr. and Ap.* **5**, 155.

Koch, R. H., Olson, E. C., and Yoss, K. M. 1965, *Ap. J.* **141**, 955.

Kopal, Z. 1972, *Ap. and Space Sci.* **17**, 161.

Kraft, R. P. 1970, in *Spectroscopic Astrophysics*, G. H. Herbig, ed. (Berkeley: University of California Press), p. 385.

Kriz, S. 1969, *Bull. Astr. Inst. Czechoslovakia* **20**, 202.

Mark, J. W.-K. 1968, *Ap. J.* **154**, 627.

McNamara, D. H. 1966, in *Spectral Classification and Multicolour Photometry, I.A.U. Symposium No. 24*, K. Loden, L. O. Loden, and U. Sinnerstad, eds. (London: Academic Press), p. 190.

Morgan, W. W., Code, A. D., and Whitford, A. E. 1955, *Ap. J. Suppl.* **2**, 41.

Morton, D. C. 1969, *Ap. J.* **158**, 629.

Morton, D. C., and Adams, T. F. 1968, *Ap. J.* **151**, 611.

Nariai, K. 1971, *Pub. Astr. Soc. Japan* **23**, 529.

Olson, E. C. 1968*a*, *Ap. J.* **153**, 187.

—— 1968*b*, *Pub. A.S.P.* **80**, 185.

Paczynski, B. 1966, *Acta Astr.* **16**, 231.

—— 1967*a*, *ibid.* **17**, 1.
—— 1967*b*, *ibid.* **17**, 355.
—— 1971, *Annual Rev. of Astr. and Astrophysics* **9**, 183.
Paczynski, B., and Ziolkowski, J. 1967, *Acta Astr.* **17**, 7.
Piotrowski, S. L. 1964, *Bull. Acad. Polonaise Sci. (Ser. Math. Astr. Phys.)* **12**, 419.
Plaut, L. 1950, *Groningen Pub.*, No. 54.
—— 1959, *Pub. A.S.P.* **71**, 167.
Plavec, M. 1967, *Bull. Astr. Inst. Czechoslovakia* **18**, 334.
—— 1968, *Advances in Astr. and Astrophysics* **6**, 201.
—— 1970, in *Stellar Rotation*, A. Slettebak, ed. (Dordrecht: D. Reidel Publishing Co.), p. 133.
—— 1973 (to be published).
Popov, M. V. 1968, *Soviet Astr.* **12**, 640.
Popper, D. M. 1943, *Ap. J.* **97**, 394.
—— 1955, *ibid.* **121**, 56.
—— 1957, *ibid.* **126**, 53.
Rachkovskaya, T. M. 1971, *Izv. Krymskoj Astrofiz. Obs.* **43**, 87.
Roman, N. G. 1951, *Ap. J.* **114**, 492.
—— 1956, *ibid.* **123**, 246.
Roy, A. E. 1952, *M.N.R.A.S.* **112**, 484.
Sackmann, I.-J., and Anand, S.P.S. 1970, *Ap. J.* **162**, 105.
Sahade, J. 1962, *Symposium on Stellar Evolution* (La Plata: Observatorio Astronomico, Universidad Nacional de la Plata), p. 185.
Slettebak, A. 1970, *Stellar Rotation* (Dordrecht: D. Reidel Publishing Co.), p. 3.
Stibbs, D. W. N. 1948, *M.N.R.A.S.* **108**, 398.
Stothers, R. 1972, *Ap. J.* **175**, 431.
—— 1973, *ibid.* (in press).
Stothers, R., and Lloyd Evans, T. 1970, *The Observatory* **90**, 186.
Stothers, R., and Lucy, L. B. 1972, *Nature* **236**, 218.
Sweet, P. A. 1950, *M.N.R.A.S.* **110**, 548.
Sweet, P. A., and Roy, A. E. 1953, *M.N.R.A.S.* **113**, 701.
van den Heuvel, E. P. J. 1970, in *Stellar Rotation*, A. Slettebak, ed. (Dordrecht: D. Reidel Publishing Co.), p. 178.
Watson, R. D. 1972, *Ap. J. Suppl.* **24**, 167.
Wood, D. B., and Forbes, J. E. 1963, *A.J.* **68**, 257.
Zahn, J.-P. 1966, *Ann. d'Ap.* **29**, 565.
Ziolkowski, J. 1969, *Ap. and Space Sci.* **3**, 14.